Probing the Cysteine-34 Position of Endogenous Serum Albumin with Thiol-Binding Doxorubicin Derivatives. Improved Efficacy of an Acid-Sensitive Doxorubicin Derivative with Specific Albumin-Binding Properties Compared to That of the Parent Compound

Felix Kratz,*,† André Warnecke,† Karin Scheuermann,† Cornelia Stockmar,† Jürgen Schwab,† Peter Lazar,† Peter Drückes,† Norbert Esser,† Joachim Drevs,† Didier Rognan,‡ Caterina Bissantz,‡,§ Caterina Hinderling,§ Gerd Folkers,§ Iduna Fichtner,|| and Clemens Unger†

Tumor Biology Center, Breisacher Strasse 117, 79106 Freiburg, Germany, CNRS, Laboratoire de Pharmacochimie de la Communication Cellulaire, UMR 7081, 74, Route du Rhin, B.P.24, F-67401 Illkirch, France, Department of Applied BioSciences, Institute of Pharmaceutical Sciences, ETH Zürich, Winterthurerstrasse 190, CH-8057 Zürich, Switzerland, and Max-Delbrück Centrum, Robert-Rössle-Strasse 10, 13122 Berlin, Germany

Received July 1, 2002

We have recently proposed a macromolecular prodrug strategy for improved cancer chemotherapy based on two features (Kratz, F.; et al. *J. Med. Chem* **2000**, *43*, 1253−1256.): (a) rapid and selective binding of thiol-reactive prodrugs to the cysteine-34 position of endogenous albumin after intravenous administration and (b) release of the albumin-bound drug in the acidic environment at the tumor site due to the incorporation of an acid-sensitive bond between the drug and the carrier. To investigate this therapeutic strategy in greater depth, four (maleinimidoalkanoyl)hydrazone derivatives of doxorubicin were synthesized differing in the length of the aliphatic spacer (**1**, $-(CH_2)_2-$; **2**, $-(CH_2)_3-$; **3**, $-(CH_2)_5-$; **4**, $-(CH_2)_7-$). The albumin-binding doxorubicin prodrugs, especially the (6-maleimidocaproyl)hydrazone derivative of doxorubicin (**3**), are rapidly and selectively bound to the cysteine-34 position of endogenous albumin. **3** was distinctly superior to the parent compound doxorubicin in three animal tumor models (RENCA, MDA-MB 435, and MCF-7) with respect to antitumor efficacy and toxicity.

Introduction

Doxorubicin is a widely used antineoplastic agent in the treatment of leukemia and lymphoma, breast and ovarian carcinoma, and many other solid tumors.[1,2] The clinical application of this anthracycline drug is, however, limited by its toxic dose-related side effects, such as myelosuppression, gastrointestinal disorders, stomatitis, cumulative cardiotoxicity, and extravasation.[1]

To circumvent these limitations and to improve the therapeutic potential of anticancer drugs, several synthetic polymers and proteins are being investigated as drug carriers.[3,4] Owing to a high metabolic turnover of tumor tissue and the enhanced vascular permeability of the blood vessels of malignant tissue for circulating macromolecules, the plasma protein albumin preferentially accumulates in solid tumors.[5] Coupling of a drug to this plasma protein is therefore a promising strategy for delivering the drug to its target site and preventing its diffusion into the healthy tissue. A number of acid-sensitive albumin and transferrin conjugates with anthracyclines have shown promising in vitro and in vivo activity.[6−10]

To achieve targeted drug delivery to tumor tissue using albumin as an *endogenous* drug carrier, we have recently proposed a macromolecular prodrug strategy based on two features:[11] (a) in situ binding of a thiol-binding prodrug to the cysteine-34 position of circulating albumin after intravenous administration; (b) release of the albumin-bound drug at the tumor site due to the incorporation of an acid-sensitive bond between the drug and the carrier.

Approximately 70% of circulating albumin in the blood stream is mercaptalbumin containing an accessible cysteine-34, which is not blocked by endogenous sulfhydryl compounds such as cysteine, homocysteine, glutathione, and nitric oxide (i.e., non-mercaptalbumin).[12−14] The free HS group of cysteine-34 of human serum albumin (HSA) is an unusual feature of an extracellular protein. To our knowledge, only three other major proteins that contain cysteine residues that are not present as interchain disulfides occur in human plasma: apolipoprotein B-100 of low-density lipoprotein (LDL) which has two cysteine residues (Cys-3734 and Cys-4190) located at the C-terminal end of the protein,[15−17] fibronectin which has two cryptic, free sulfhydryl groups,[18,19] and α_1-antitrypsin which has a single cysteine residue (Cys-232).[20−22] The sulfhydryl groups in these proteins do not react readily with sulfhydryl reagents under physiological conditions and are normally linked to either cysteine or glutathione in the blood circulation.[15−22]

* To whom correspondence should be addressed. Address: Department of Medical Oncology, Clinical Research, Tumor Biology Center, Breisacher Strasse 117, D-79106 Freiburg, Germany. Phone: 0049-761-2062176. Fax: 0049-761-2061899. E-mail: felix@tumorbio.uni-freiburg.de.

† Tumor Biology Center.

‡ Laboratoire de Pharmacochimie de la Communication Cellulaire.

§ Institute of Pharmaceutical Sciences.

|| Max-Delbrück Centrum.

10.1021/jm020276c CCC: $22.00
Published on Web 11/09/2002

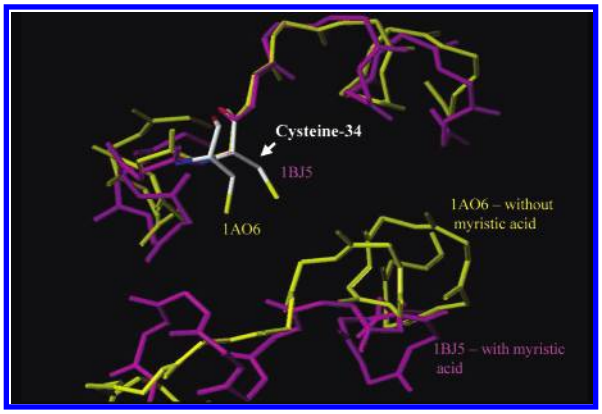

Figure 1. Three-dimensional structure of the cysteine-34 binding pocket of HSA according to the X-ray structure of the defatted protein structure (PDB entry 1ao6) and the albumin structure in which five molecules of myristic acid are bound (PDB entry 1bj5).

The concentration of low molecular weight sulfhydryl compounds in human blood plasma in their reduced form, i.e., cysteine (∼10−12 μM),[23,24] homocysteine (∼0.15−0.25 μM),[23,24] cysteinylglycine (∼3−4 μM),[23−26] or glutathione (∼4−5 μM),[23,24,26] is low when compared to the total thiol concentration in human plasma, which is in the range 400−500 μM according to the literature and our own investigations.[27,28] The free thiol group at the cysteine-34 position of HSA accounts for the major amount of the total thiol concentration (80−90%) in blood plasma.

Finally, the HS group of cysteine-34 of HSA is the most reactive thiol group in human plasma because of the low pK_a of Cys-34 in HSA, which is approximately 7 compared to 8.5 and 8.9 for cysteine and glutathione, respectively.[29]

Taken together, the HS group of cysteine-34 of HSA is a unique and accessible functional group of a plasma protein that could be exploited for in situ coupling of a thiol-reactive prodrug to circulating albumin after intravenous administration. The cysteine-34 position of HSA is located in subdomain IA. The X-ray structure of the defatted protein structure (PDB entry 1ao6 [30]) reveals that cysteine-34 is located in a hydrophobic crevice on the surface of the protein that is approximately 10−12 Å deep (see Figure 1). When HSA is complexed with long-chain fatty acids as in the X-ray structure in which five molecules of myristic acid are bound (PDB entry 1bj5), the crevice is opened up, exposing the HS group of cysteine-34 (see Figure 1).

In our earlier work, we showed that an acid-sensitive (maleimidophenylacetyl)hydrazone derivative of doxorubicin bound preferentially and rapidly to cysteine-34 of endogenous albumin and demonstrated superior antitumor efficacy in murine renal cell carcinoma compared to doxorubicin.[11]

The objective of this work was to study the interaction of thiol-binding doxorubicin derivatives with exogenous and endogenous albumin in greater depth and to compare their in vitro and in vivo activity with that of doxorubicin. Considering the geometry of the crevice at the cysteine-34 position of HSA, we selected four doxorubicin derivatives for our investigations (Figure 2) that differ in the length of the aliphatic side chain in the maleimide spacer.

Results

Doxorubicin derivatives **1**−**5** were synthesized according to published procedures;[31,32] characterization data are listed in the Experimental Section.

A. Kinetics of Binding of 1−4 to the Cysteine-34 Position of HSA. Fluorescence polarization is a suitable technique for studying the interaction of fluorescent substrates and macromolecules. Owing to the fluorescent chromophor of doxorubicin, **1**−**4** were incubated with HSA at pH 7.4 at room temperature in the presence and absence of myristic acid, and the change in fluorescence polarization was monitored over time. The binding curves are shown in Figure 3 in Supporting Information. The reaction of maleimides with sulfhydryl groups follows second-order kinetics,[33] and all binding curves could be fitted to an equation for second-order kinetics (see Experimental Section for details). The second-order rate constants k_2 for the reactions of **1**−**4** with the cysteine-34 position of HSA are listed in Table 1 and are in the range 600−2250 L mol^{-1} min^{-1}. **3** showed the highest rate constant in the presence of 5 equiv of myristic acid but not when commercially available albumin that contained approximately 1 equiv of fatty acids was used.

For all of the following studies, we selected **3** as a candidate for investigating our therapeutic approach in detail.

B. Molecular Modeling. Modeling the covalent interaction of **3** with the myristic acid bound albumin X-ray structure (PDB entry 1bj5) suggests that the optimal length of the polymethylene spacer consists of five carbon atoms (Figure 4). The polymethylene spacer interacts with the hydrophobic channel at the cysteine-34 position of HSA and places hydrophilic moieties of **3** (hydrazone group, alcoholic moiety) at the opening of the hydrophobic channel in such a way that they are able to interact through H bonds with polar amino acid residues (Glu 43, Lys 73, Thr 76).

C. Albumin-Binding Properties of 3. C.1. Binding of 3 to Exogenous Human Serum Albumin. The sulfhydryl group of cysteine-34 of HSA adds to the double bond of the heterocycle's Michael system of **3**, forming a stable thioether bond. Figure 5 shows the chromatographic profile of a reverse-phase system for an incubation study of **3** with HSA after 5 and 90 min at 37 °C. The major amount of **3** reacts with HSA within the first 5 min and is observed as a peak eluting at ∼36 min when detected at 495 nm. The reaction of **3** with HSA is specific for the HS group of cysteine-34. When this position is blocked with an excess of *N*-ethylmaleimide (NEM) prior to incubation with **3**, only marginal binding to HSA occurs even after 90 min (see Figure 5). Furthermore, when (6-succinimidocaproyl)hydrazone of doxorubicin (**5**) is incubated with HSA, which does not contain the thiol-reactive double bond of the maleimide group, no binding to HSA is observed (see Figure 5), demonstrating that strong physical interactions of the doxorubicin spacer structure with HSA are negligible. A similar result is obtained when doxorubicin is incubated with HSA (see Figure 5).

When the albumin conjugate of **3** is prepared by reacting commercially available albumin that contains approximately 30% mercaptalbumin with **3**, mass spectrometry of the isolated conjugate showed that the mass

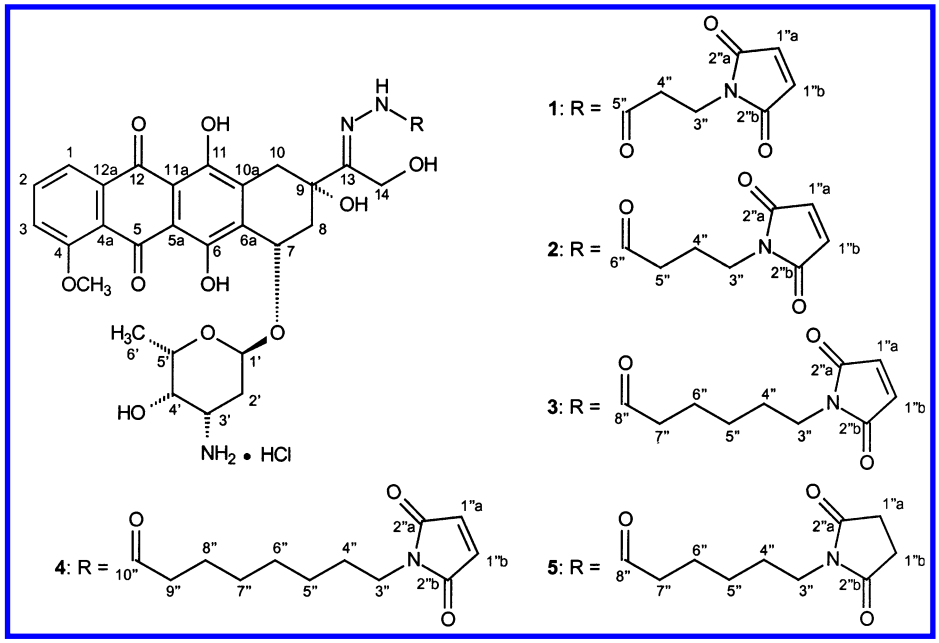

Figure 2. General structure of doxorubicin hydrazone derivatives (**1**−**5**) containing aliphatic maleimide spacers.

Table 1. Second-Order Rate Constants (pH 7.4 at Room Temperature) for the Reaction of **1**−**4** with HSA in the Absence or Presence of 5 Equiv of Myristic Acid ($v = k_2$[HSA-Cys34-SH][**1**−**4**])[a]

compound	k_2 with HSA (L mol^{-1} min^{-1})	k_2 with HSA in the presence of 5 equiv of myristic acid (L mol^{-1} min^{-1})
1	1430 ± 15; $r = 0.996$	1070 ± 20; $r = 0.989$
2	1510 ± 15; $r = 0.990$	1140 ± 10; $r = 0.999$
3	1040 ± 10; $r = 0.986$	2250 ± 50; $r = 0.991$
4	600 ± 40; $r = 0.970$	960 ± 30; $r = 0.970$

[a] Similar results were obtained in a further independent experiment.

peak of mercaptalbumin practically disappears (66 437 Da) and shifts to ∼67 186 Da, which corresponds approximately to the sum of the principal mass of mercaptalbumin and the mass of **3** (see Figure 6 in Supporting Information).

C.2. Binding of 3 to Endogenous Albumin in Human Plasma. To determine the coupling rate and selectivity of **3** for endogenous albumin, **3** was incubated with human blood plasma at 37 °C and the samples were subsequently analyzed by reverse-phase chromatography. Chromatograms after an incubation time of 2, 5, and 90 min are shown in Figure 7. Protein components were detected at 280 nm, and the anthracycline moiety was detected simultaneously at 495 nm. Coupling of **3** to endogenous albumin is almost complete after 2 min, with the major amount of **3** associated with the albumin peak, which elutes at ∼36 min. When this peak is isolated and analyzed by mass spectrometry (ESI), the mass spectrum reveals that the mass peak for the molecular weight of mercaptalbumin (66 433 Da) is shifted to a higher mass (67 183 Da) corresponding to the albumin-bound form of **3** (see Figure 8 in Supporting Information).

The following experiment was carried out to demonstrate that the cysteine-34 position of albumin is involved in the coupling step. Human plasma was preincubated with an excess of a nonfluorescent maleimide with respect to the albumin concentration in the blood plasma, i.e., 6-maleimidocaproic acid (EMC), before adding **3**. The resulting chromatogram (see Figure 7) shows that in this case only marginal binding of **3** to albumin takes place, and the major amount of **3** elutes with a retention time of ∼12 min. Furthermore, no additional binding to other plasma proteins is observed after an incubation period of 90 min.

In contrast to **3**, 6-(succinimidocaproyl)hydrazone of doxorubicin (**5**) and doxorubicin showed only marginal binding to endogenous plasma albumin even after an incubation time of 90 min (see Figure 7).

C.3. Binding Properties of 3 in Human Blood. Incubation studies of **3** with human blood and subsequent HPLC analysis of the resulting blood plasma after centrifugation led to similar chromatographic profiles as noted with human plasma (chromatogram in Figure 9 of Supporting Information).

The distribution of **3** or doxorubicin to the plasma or blood cell compartment in whole blood was studied by incubating the drug with human blood at 37 °C over a period of 60 min. After centrifugation, the anthracycline content was determined photometrically at 495 nm. Figure 10 depicts the absorption values for **3** or doxorubicin in the plasma phase over 60 min. The diagram shows that **3** is almost completely distributed in the plasma phase (approximately 90%) in comparison to doxorubicin (approximately 30%) after 60 min. This result indicates that the interaction of **3** with blood cells is secondary and that the major amount of **3** is present in the plasma phase, primarily in its albumin-bound form. In contrast, doxorubicin apparently diffuses into blood cells over time under the chosen experimental conditions.

C.4. Stability of 3 Bound to the Cysteine-34 Position of HSA in Human Plasma and in Cell Culture Medium. As described above, **3** is quantitatively bound to endogenous albumin within a few minutes. Figure 11 in Supporting Information shows the chromatographic profiles of **3** bound to albumin in human plasma after 90 min and 24 h at 37 °C. Within 24 h, only very small amounts of released doxorubicin are observed and the initial peak of **3** bound to albumin

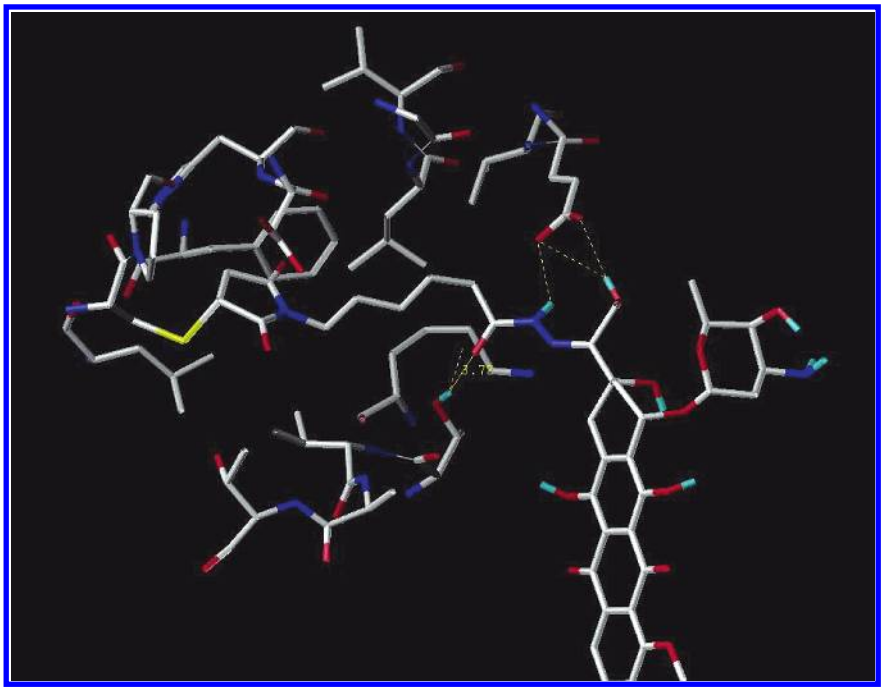

Figure 4. By use of the docking program FlexX, hexylmaleimide was docked as close to the thiol group of the Cys-34 of HSA (PDB entry 1bj5, myristic acid form) as possible, the maleimide was covalently linked to Cys-34, and the structure was minimized (first in vacuo and then with a water shell). Starting from the minimized structure, a molecular dynamic simulation was carried out over 100 ps. After this time, equilibrium was reached. Doxorubicin and the hydrazone bond were covalently linked to the hexylmaleimide group and then fitted manually. The hydrophobic spacer fits neatly in the Cys-34 pocket, allowing the hydrazone group and doxorubicin to form hydrogen bonds with polar amino acid side chains (H bonds are indicated as yellow dashed lines).

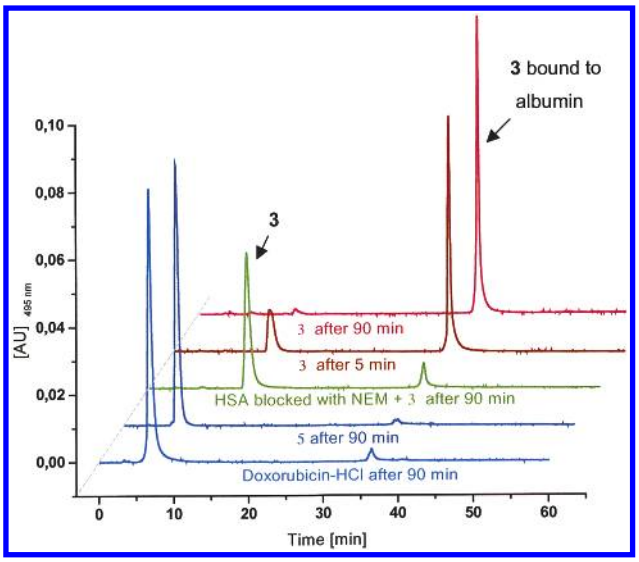

Figure 5. Chromatograms of incubation studies of human serum albumin [and human serum albumin preincubated with *N*-ethylmaleimide (NEM)] with **3**, **5**, and doxorubicin at 37 °C. Concentration of the anthracycline was 100 μM. For chromatographic conditions, see Experimental Section.

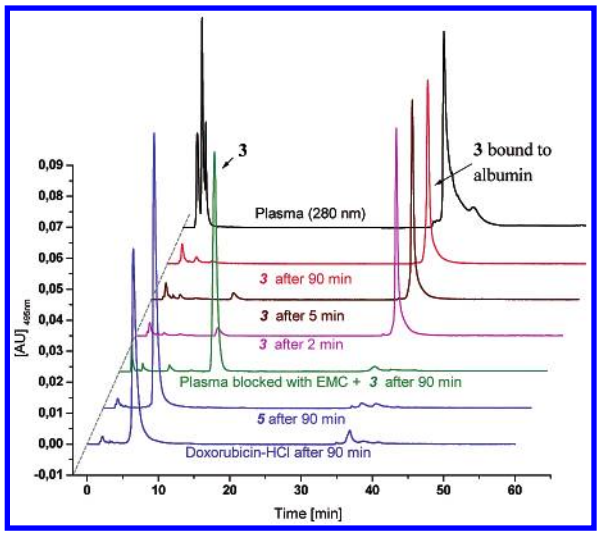

Figure 7. Chromatograms of incubation studies of human plasma [and human plasma preincubated with 6-maleimidocaproic acid (EMC)] with **3**, **5**, and doxorubicin at 37 °C. Concentrations of the anthracycline was 100 μM. For chromatographic conditions, see Experimental Section.

remains almost unchanged, demonstrating that the liberation of doxorubicin in human plasma is marginal. Similar results were obtained when the albumin conjugate with **3** was incubated with cell-conditioned medium from MCF-7 cells, demonstrating that only small traces of doxorubicin are released extracellularly under conditions prevailing in cell culture experiments (see below).

C.5. Acid-Sensitive Properties of 3 Bound to the Cysteine-34 Position of Human Serum Albumin. To assess the acid lability of the albumin conjugate of **3**, the conjugate was incubated at pH 5.0 at 37 °C and analyzed over a period of 3 h on a C-18 reverse-phase column. The initial peak of albumin conjugate of **3** decreased rapidly with a concomitant appearance of the peak for doxorubicin. The half-life was determined as ~25 min (see Figure 12 in Supporting Information).

D. In Vitro Studies with 3. D.1. Antiproliferative Activity of 3 and Derivatives against Three Tumor Cell Lines. The antiproliferative activity of **3**, of the albumin conjugate of **3**, of (6-succinimidocaproyl)hydrazone of doxorubicin (**5**), and of free doxorubicin were assessed in the following three tumor cell lines using

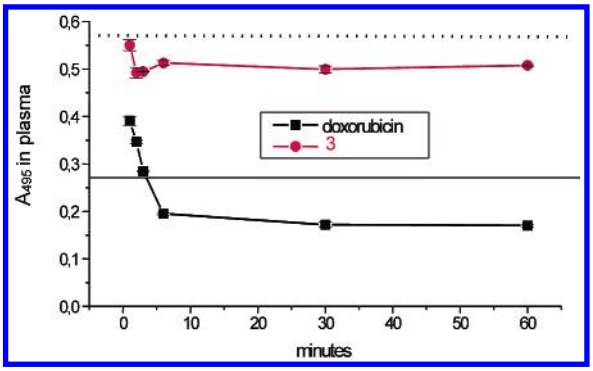

Figure 10. Concentrations of doxorubicin and **3** in the plasma phase after incubating the drugs for up to 60 min with whole blood at 37 °C: (- - -) maximum theoretical concentration of anthracycline in the plasma phase assuming that the anthracycline is distributed 100% in the plasma phase; (−) theoretical concentration of anthracycline in the plasma phase assuming that the anthracycline is equally distributed in human blood between plasma and blood cells. Doxorubicin or **3** was added to human blood samples to a final concentration of 225 μM. After an incubation time of t = 0, 1, 2, 3, 6, 30, and 60 min, each sample was centrifuged (duration: 20−30 s), the plasma phase was diluted with sodium phosphate buffer (4 mM Na_2HPO_4 and 0.15 M NaCl, pH 7.4), and the concentration of anthracycline was measured photometrically at 495 nm against a plasma reference without the drug. The averages of three absorption values at 495 nm are depicted in the diagram against the time scale.

Table 2. IC_{50} Values (μM)[a] for Doxorubicin, **3**, the Albumin Conjugate of **3**, and **5** in RENCA, MCF-7, and LXFL529 Tumor Cells as Determined with the BrdU-Incorporation Assay

compound	IC_{50} in RENCA cells (μM)	IC_{50} in MCF-7 cells (μM)	IC_{50} in LXFL529 cells (μM)
doxorubicin	0.05 ± 0.02	0.04 ± 0.02	0.04 ± 0.02
5	0.7 ± 0.2	1.1 ± 0.1	0.5 ± 0.2
3	1.0 ± 002	1.1 ± 0.1	0.5 ± 0.1
albumin conjugate of **3**	0.9 ± 0.3	1.0 ± 0.1	0.4 ± 0.1

[a] IC_{50} values (50% inhibitory concentration) represent the mean ± standard deviation (n = 4). Similar results were obtained in a further independent experiment.

the 5-bromo-2′-deoxyuridine (BrdU) incorporation assay: MCF-7 human mamma carcinoma, LXFL529 human lung carcinoma, and RENCA murine renal cell carcinoma. The IC_{50} values that were obtained after a 48 h cell exposure are summarized in Table 2.

Doxorubicin has a strong inhibitory effect on DNA synthesis in all three cells with an IC_{50} value in the range 0.04−0.05 μM. **3**, **5**, and the albumin conjugate of **3** are less active in the three cell lines but still exhibit IC_{50} values in the low micromolar range (0.4−1.0 μM).

D.2. Intracellular Release of Doxorubicin. To determine whether doxorubicin is released intracellularly after cellular uptake of the albumin conjugate of **3**, the conjugate was incubated with MCF-7 tumor cells for 6, 16, and 24 h. Cells were lysed by ultrasonication, and doxorubicin was extracted into an organic phase and subsequently analyzed by reverse chromatography using fluorescence detection (see Experimental Section for details). Figure 13 in Supporting Information shows chromatograms of the extracted samples. Doxorubicin is the major product that can be detected after the extraction step, and the amount of doxorubicin increases with time. The ratio of the peak area of doxorubicin to the amount of cells present at the individual time points

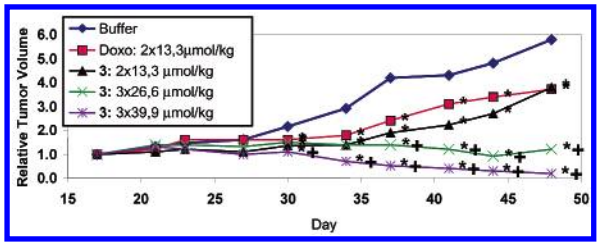

Figure 15. Curves depicting tumor growth inhibition of subcutaneous breast carcinoma MDA-MB-435 xenografts under therapy with doxorubicin and **3**: (∗) significant to buffer; (+) significant to doxorubin. The dosages (iv) are the following: doxorubicin, 2 × 13.3 μmol (=2 × 8 mg/kg doxorubicin); **3**, 2 × 13.3 μmol (=2 × 8 mg/kg doxorubicin equivalents), 3 × 26.6 μmol (=3 × 16 mg/kg doxorubicin equivalents), 3 × 39.9 μmol (=3 × 24 mg/kg doxorubicin equivalents).

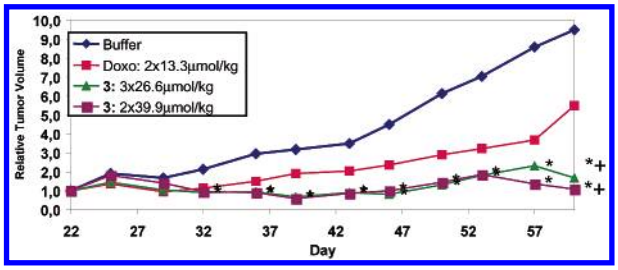

Figure 16. Curves depicting tumor growth inhibition of subcutaneous breast carcinoma MCF-7 xenografts under therapy with doxorubicin and **3**: (∗) significant to buffer; (+) significant to doxorubin. The dosages (iv) are the following: doxorubicin, 2 × 13.3 μmol (=2 × 8 mg/kg doxorubicin); **3**, 3 × 26.6 μmol (=3 × 16 mg/kg doxorubicin equivalents), 2 × 39.9 μmol (=3 × 24 mg/kg doxorubicin equivalents).

increases with time, indicating that increasing amounts of doxorubicin accumulate in MCF-7 tumor cells (Figure 14 in Supporting Information).

E. In Vivo Activity of 3. **3** was evaluated in two nude mice models (MDA-MB 435, MCF-7) and one orthotopic model (murine renal cell carcinoma model RENCA) in a strict comparison to the parent compound doxorubicin. Preliminary toxicity studies in nude mice showed that the maximum tolerated dose of **3** was approximately 4 times higher than for free doxorubicin.

In the MDA-MB 435 model, the antitumor efficacy of **3** was compared to that of doxorubicin at the following doses: doxorubicin, 2 × 13.3 μmol (=2 × 8 mg/kg doxorubicin); **3**, 2 × 13.3 μmol (=2 × 8 mg/kg doxorubicin equivalents), 3 × 26.6 μmol (=3 × 16 mg/kg doxorubicin equivalents), and 3 × 39.9 μmol (=3 × 24 mg/kg doxorubicin equivalents). The results of this animal experiment are shown in Figure 15 (body weight change, *T*/*C* values, and blood cell parameters are in Table 3 in Supporting Information). At the optimal dose of free doxorubicin (2 × 13.3 μmol/kg), a moderate inhibition in tumor growth is observed with **3**, comparable to the effect of free doxorubicin at the same dose. At higher doses (3 × 26.6and 3 × 39.9 μmol/kg), therapy with **3** is well tolerated, producing good antitumor effects at 3 × 26.6 μmol/kg and complete remissions at 3 × 39.3 μmol/kg.

In the MCF-7 model, the optimal dose for free doxorubicin (2 × 13.3 μmol/kg) produced a moderate but nonsignificant inhibition in tumor growth (see Figure 16). In contrast, therapy with **3** (3 × 26.6and 2 × 39.9 μmol/kg) was well tolerated, producing a significant antitumor effect with no increase in tumor growth

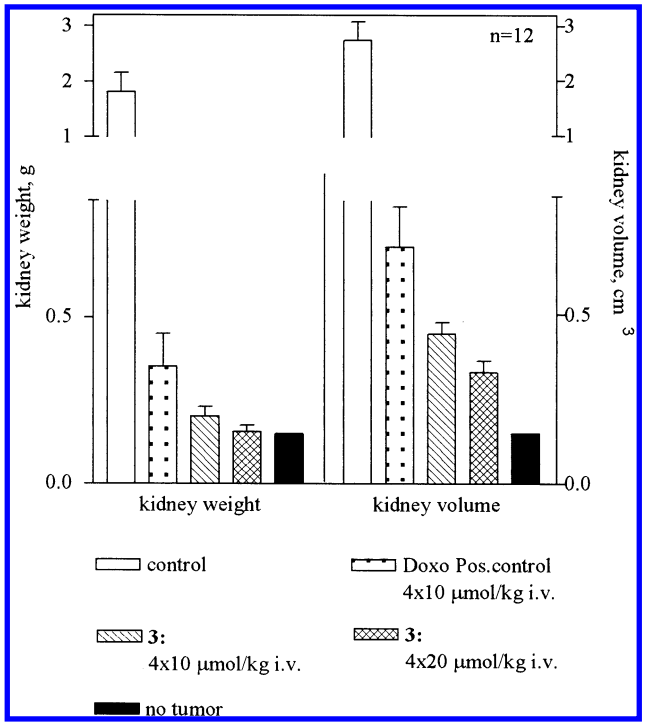

Figure 17. Therapeutic effects of doxorubicin and **3** on kidney weight and volume compared to the control group in the RENCA model; $p < 0.05$ ($n = 12$).

compared to the initial size of the subcutaneously established tumors (body weight change, *T*/*C* values, and blood cell parameters are in Table 4 in Supporting Information). WBC counts in the groups treated with **3** were lower than for the doxorubicin-treated group.

In the RENCA model, the subcapsular renal injection of RENCA cells in a syngenic BALB/c mouse is followed by the progressive development of a primary tumor mass in the left kidney. One week after application, the primary tumor is macroscopically visible. Twelve animals per group were used for the experiment. Therapy was initiated by intravenous application of a single dose of 4 × 10 μmol/kg doxorubicin (=4 × 6 mg/kg doxorubicin) and of 4 × 10 μmol/kg of **3** (=4 × 6 mg/kg doxorubicin equivalents) or 4 × 20 μmol/kg of **3** (=4 × 12 mg/kg doxorubicin equivalents) on days 10, 14, 17, and 21 after renal application of RENCA cells (day 1). Primary tumors were evaluated on day 24.

The therapeutic effects of doxorubicin and **3** on kidney tumor volume and weight are shown in Figure 17 in comparison to a control group receiving buffer. After 24 days, mice in the doxorubicin-treated group showed distinct kidney tumors, which is reflected by a significant increase in kidney weight and kidney volume compared to healthy kidneys. In the group treated with **3** at the identical dose, both kidney volumes and weights increased to a slightly lesser extent, and at a dose of 4 × 20 μmol/kg they increased to a much lesser extent compared to healthy kidneys. Thus, considerable reduction in tumor size occurred. Representative photographic images of the left (RENCA) and right (healthy) kidneys for six animals of the doxorubicin group (4 × 10 μmol/kg) and the group treated with **3** (4 × 20 μmol/kg) are depicted in Figure 18 in Supporting Information.

Table 5 lists the number of complete and partial remissions as well as the number of nonresponders per group based on the following criteria: kidney weight 0.1−0.15 g ⇒ complete remission (CR) (corresponds to the average weight of a healthy kidney); kidney weight 0.16−1.00 g ⇒ partial remission (PR); kidney weight > 1.00 g ⇒ nonresponder (NR).

Table 5. Number of Complete (CR) and Partial Remissions (PR) as Well as the Number of Nonresponders (NR) per Group in Kidney Tumor-Bearing Mice Treated with Doxorubicin or **3**[a]

group, first experiment	CR	PR	NR
doxorubicin (4 × 10 μmol/kg)	4	6	2
3 (4 × 10 μmol/kg)	5	7	
3 (4 × 20 μmol/kg)	9	3	

group, second experiment	CR	PR	NR
doxorubicin (4 × 20 μmol/kg) 92% mortality		1	
3 (4 × 10 μmol/kg)	4	8	
3 (4 × 20 μmol/kg)	9	3	

[a] Kidney weight 0.1−0.15 g ⇒ complete remission (CR) (corresponds to the average weight of a healthy kidney); kidney weight 0.16−1.00 g ⇒ partial remission (PR); kidney weight >1.00 g ⇒ nonresponder (NR).

At both doses (4 × 10 and 4 × 20 μmol/kg), the therapeutic results with **3** are better than those obtained with doxorubicin at 4 × 10 μmol/kg with respect to the number of complete and partial responses. At 4 × 20 μmol/kg, **3** produced complete remissions in 9 of the 12 treated mice.

A noteworthy finding of the experiment is the change in body weight observed in the different groups (see Figure 19 in Supporting Information). Whereas therapy with doxorubicin at a dose of 4 × 10 μmol/kg produced a significant decrease in overall body weight (about −10%, days 0−24), therapy with **3** at doses of 4 × 10 or 4 × 20 μmol/kg did not produce an overall change in body weight after the 24 days. This indicates that **3** is extremely well tolerated in accordance with the data in the nude mice model MDA-MB 435.

The experiment with doxorubicin and **3** in the RENCA model was repeated, but this time doxorubicin was administered at twice the dose of the first experiment, i.e., 4 × 20 μmol/kg. **3** was again administered at 4 × 10 and 20 μmol/kg (kidney tumor volume and weights as well as body weight curves of this experiment are in Figures 20 and 21 in Supporting Information). Table 5 lists the number of complete and partial remissions as well as the number of nonresponders per group observed in this experiment. Doxorubicin therapy at a dose of 4 × 20 μmol/kg is highly toxic. A total of 11 of the 12 treated animals died between days 17 and 21. In comparison, as observed in the first experiment, therapy with **3** at doses of 4 × 10 and 20 μmol/kg produced no mortality and a significant reduction in tumor growth compared to the untreated group with complete remissions in 9 of the 12 treated mice at 4 × 20 μmol/kg. Again, no body weight change was observed with **3** at doses of 4 × 10 and 20 μmol/kg at the end of the experiment.

Discussion

The pathophysiology of tumor tissue, characterized by angiogenesis, hypervasculature, a defective vascular architecture, and an impaired lymphatic drainage, seems to be a universal feature of solid tumors that can be exploited for tumor-selective drug delivery using macromolecules as drug carriers.[34] A number of cleav-

able drug conjugates with synthetic polymers have been developed for this purpose, and first candidates such as PK1 (doxorubicin conjugated with *N*-(2-hydroxypropyl)methacrylamide copolymer)[35] or Prothecan (camptothecin conjugated with poly(ethylene glycol))[36] are undergoing clinical trials.

There is meanwhile a large body of evidence available demonstrating that the plasma proteins albumin and transferrin accumulate in experimental solid tumors.[5] Thus, we have previously developed acid-sensitive doxorubicin conjugates with albumin and transferrin that demonstrated superior in vivo activity compared to the parent compound.[9,10] Interestingly, we found no pronounced difference between identically constructed transferrin and albumin doxorubicin conjugates with regard to in vitro or in vivo efficacy.[9]

As a consequence, we focused our work on a prodrug concept that exploits endogenous albumin as the drug carrier in which a thiol-binding prodrug is selectively bound to the cysteine-34 position of circulating albumin.[11] We reasoned that exploiting endogenous albumin as a drug carrier would have several advantages over ex vivo synthesized drug albumin conjugates: (a) the use of commercial and possibly pathogenic albumin is avoided; (b) albumin-binding drugs are chemically well-defined and based on straightforward organic chemistry; (c) albumin-binding drugs are fairly simple and inexpensive to manufacture compared to ex vivo synthesized drug albumin conjugates; (d) a broad range of drugs for developing albumin-binding drugs can be used; the analytical requirements for defining the pharmaceutical products are comparable to those of any other organic drug candidate.

In this work, we selected the maleimide doxorubicin hydrazone derivatives **1**−**4** for our investigations. **1**−**4** contain an acid-sensitive hydrazone linker that allows doxorubicin to be released either extracellularly in the slightly acidic environment often present in tumor tissue or intracellularly in acidic endosomal or lysosomal compartments after cellular uptake of the conjugate by the tumor cell. The carboxylic hydrazone linker was initially designed for conjugating doxorubicin to monoclonal antibodies.[37,38]

Fluorescence polarization studies showed that **1**−**4** were rapidly bound to the cysteine-34 position of HSA with second-order rate constants in the range 600−2250 L mol^{-1} min^{-1}. Differences in the rate constants were noted in the absence or presence of myristic acid. When HSA is complexed with long-chain fatty acids, the crevice is opened up, exposing the HS group of cysteine-34 (see Figure 1). In human plasma, circulating albumin is generally complexed with one to three molecules of long-chain fatty acids.[30] **3** demonstrated the highest rate second-order rate constant for HSA in the presence of myristic acid. Molecular modeling studies with **3** bound to the cysteine-34 position of the X-ray structure in which five molecules of myristic acid are bound showed that the aliphatic spacer fitted neatly into the hydrophobic crevice, and the adjacent hydrazone bond and CH_2OH group of doxorubicin were able to interact with amino acids on the surface of the cysteine-34 pocket through hydrogen bonds (see Figure 4). This theoretical result indicates that **3** bound to the cysteine-34 position of HSA is stabilized with regard to potential hydrolysis. Incubation studies in human plasma and cell culture medium confirmed this assumption with only traces of doxorubicin being liberated from the albumin conjugate with **3** after 24 h at 37 °C (see Figure 11 in Supporting Information).

According to our incubation studies in human blood and plasma, **3** was bound selectively to endogenous albumin within minutes. Minor side reactions with other plasma components that are likely to occur owing to the complexity of blood plasma were observed as peaks eluting at short retention times on our reverse-phase HPLC system (see Figure 3 in Supporting Information). Binding of **3** to blood cells does not appear to be a major issue (see Figure 10).

On the cellular level, **3** and the albumin conjugate of **3** demonstrated IC_{50} values in three tumor cell lines in the low micromolar range (0.4−1.0 μM) that were approximately an order of magnitude higher than those for doxorubicin (see Table 2). This is perhaps not surprising considering that a short-term assay (over 48 h) was used and the cellular uptake of the albumin-bound form of **3** and concomitant intracellular accumulation of doxorubicin will be different from that of doxorubicin. Incubation studies with the albumin conjugate of **3** in MCF-7 cells showed that increasing amounts of doxorubicin are released intracellularly with time (Figures 13 and 14 in Supporting Information). Confocal laser scanning microscopy studies with related acid-sensitive albumin doxorubicin conjugates have demonstrated that besides the cell nucleus, the mitochondria and golgi compartments are important sites of accumulation and interaction for intracellularly released doxorubicin.[39]

3 was superior to free doxorubicin, the clinical standard, in a murine renal cell carcinoma model (RENCA) and in two mamma carcinoma xenograft models in nude mice (MDA-MB 435, MCF-7) with regard to antitumor efficacy and toxicity. Complete remissions were achieved with **3** in the RENCA and MDA-MB 435 models, in contrast to therapy with doxorubicin.

In the initial work regarding acid-cleavable linkers of doxorubicin, **3** was coupled to a chimeric human or mouse monoclonal antibody that is specific for Lewis Y, an antigen that is abundantly expressed on the surface of several human carcinomas.[38] The BR96 doxorubicin immunoconjugate, in which approximately eight doxorubicin molecules are coupled to the antibody, has shown high antitumor activity in a number of xenograft tumor models compared to unbound doxorubicin.[38,40] It is difficult to weigh precisely the preclinical data of this immunoconjugate with the data presented in this work considering that a different loading ratio and different tumor models were used. What can be inferred is that both formulations were superior to doxorubicin and were able to induce complete remissions in the tumor models studied. Furthermore, the doses needed to achieve complete remissions were higher for **3** than for the BR96 doxorubicin immunoconjugate.

It should be noted that equivalent doses of **3** and doxorubicin did not produce a significant difference in antitumor response but only in toxicity. The mechanism by which macromolecules such as serum proteins accumulate in tumor tissue has been termed enhanced permeability and retention of macromolecules ("EPR

effect") and serves as a working model for explaining the targeting potential of macromolecules for solid tumors.[34] Our data suggest that at equivalent doses using a 3-day or weekly dose schedule comparable amounts of pharmacologically active doxorubicin reach the cells of the tumor when tumor-bearing mice are treated with either doxorubicin or the prodrug **3**.

A major difference between doxorubicin and **3** is the substantial increase in the maximum tolerated dose (MTD). Toxicity studies in mice, rats, and dogs have meanwhile shown that the MTD of **3** is 3- to 4-fold higher than for doxorubicin. As a consequence, the therapeutic index of **3** is significantly enhanced, allowing high doses to be administered to tumor-bearing animals, with a concomitant increase in antitumor activity compared to that of free doxorubicin. Generally, a high degree of protein binding, especially to albumin, is considered a disadvantage because only the free drug can exert its pharmacological effect. In situ binding of prodrugs to albumin turns this potential disadvantage into a therapeutic benefit by incorporating a cleavable bond between the drug and the albumin-binding moiety that ensures a specific release of the drug at its site of action. By distribution of the drug in its albumin-bound form in the body, the natural detoxifying functions of endogenous albumin are temporarily exploited for improving the safety and efficacy of the drug.

The BR96 doxorubicin immunoconjugate has recently been evaluated in phase I and II studies.[41] Unfortunately, the immunoconjugate showed only limited antitumor activity in metastatic breast cancer and also induced severe gastrointestinal toxicity, which is probably due to cross-reactivity with the respective normal tissue expressing the target antigen.

Whether **3** is able to circumvent such disadvantages in humans needs to evaluated; a phase I study with **3** is being planned at present.

Experimental Section

A. Chemicals, Materials, and Spectroscopy. Doxorubicin hydrochloride (M_r = 580.0) was purchased from Hande Tech Development Co. USA, Inc., and organic solvents were HPLC grade (Merck, FRG) or a gift from BASF AG. All other chemicals used were at least reagent grade and obtained from Sigma-Aldrich (Deisenhofen, FRG) or Merck (Darmstadt, FRG) and used without further purification. Human serum albumin (20% solution) was purchased from Dessau Pharma, FRG, and contained approximately 30% free thiol groups as assessed with Ellmann's test. The buffers used were vacuum-filtered through a 0.2 μm membrane (Sartorius, FRG) and thoroughly degassed with argon or nitrogen prior to use. Cell culture media, supplements (L-glutamine, antibiotics, trypsin versene/EDTA), and fetal calf serum (FCS) were purchased from Bio Whittaker (Serva, Heidelberg, FRG). All culture flasks were obtained from Greiner Labortechnik (Frickenhausen, FRG).

^{13}C NMR data were obtained with a Bruker ARX 300 (internal standard is TMS). Mass spectrometry data were obtained with a Finnigan-MAT 312, and analytical HPLC measurements were performed with a Kontron 422 pump and a Kontron 535 detector (at 218 or 495 nm). For peak integration, the KromaSystem 2000 software (version 1.83 by Kontron BioTEK) was used: column, Waters, 100 Å, Symmetry C18 [4.6 mm × 250 mm]; flow, 1.0 mL/min; mobile phase, 30% CH_3-CN, 70% 20 mM potassium phosphate (pH 7.0). UV−vis spectrophotometry was carried out with a double-beam spectrophotometer U-2000 from Hitachi. Mass spectrometry (LC−ESI-MS) was performed by A&M GmbH, Bergheim, FRG, using a Chrom-Sil butyl-2FE C4 column (300 Å, 5 μm, 10 mm × 2 mm) and a LCQ Classic ion trap (ThermoQuest): capillary voltage, 11−20 V; spray voltage, 4 V.

For incubation studies, **3** was dissolved in a sterile isotonic buffer containing 10 mM sodium phosphate and 5% D-glucose (pH 6.4) at a concentration of 5.4 mg/mL. In the animal experiments, a sterile isotonic buffer containing 4 mM sodium phosphate and 0.15 M sodium chloride (pH 6.5) was used. Albumin concentration were determined with a Vitros analyzer from Ortho-clinical Diagnostics.

B. Characterization of 1−5. 1. HPLC (Symmetry C18, 495 nm): purity >95%. ESI-MS (4.0 kV, methanol): *m*/z (%) 709.3 ([M + H]$^+$, 100). ^{13}C NMR (DMSO-d_6): δ 16.66 (C6′), 29.99 (C2′), 31.82 (C10), 33.65 (C4″), 46.50 (C3′), 55.96, 56.52, 65.91, 66.18, 71.74, 72.18 (OCH_3, C7,9,14,4′,5′), 98.81 (C1′), 110.44 (C5a/11a), 119.02, 119.62, 119.96 (C1,3,4a), 134.30 (C1″a/1″b), 134.49, 135.53, 136.10, 136.27 (C2,6a,10a,12a), 153.35, 154.03, 156.47 (C6,11,13), 160.69 (C4), 170.49 (C2″a/2″b), 173.91 (C5″), 186.39 (C5/12).

2. HPLC (Symmetry C18, 495 nm): purity >95%. ESI-MS (4.0 kV, methanol): *m*/z (%) 723.3 ([M + H]$^+$, 42). ^{13}C NMR (DMSO-d_6): δ 16.69 (C6′), 22.71 (C4″), 28.48 (C2′), 30.46 (C10), 33.45 (C5″), 36.62 (C3″), 46.52 (C3′), 56.06, 56.50, 65.93, 66.20, 71.53, 72.12 (OCH_3, C7,9,14,4′,5′), 98.85 (C1′), 110.45, 110.49 (C5a,11a), 118.87, 119.56, 119.90 (C1,3,4a), 134.21 (C1″a/1″b), 134.37, 134.59, 135.60, 136.10 (C2,6a,10a,12a), 153.03, 154.19, 156.32 (C6,11,13), 160.69 (C4), 170.74 (C2″a/2″b), 173.13 (C6″), 186.30, 186.37 (C5,12).

3. HPLC (Symmetry C18, 495 nm): purity >95%. ESI-MS: *m*/z (%) 751.2 ([M + H]$^+$, 45). ^{13}C NMR (DMSO-d_6): δ 16.71 (C6′), 23.35, 25.74, 27.64, 27.95 (C2′,4″-6″), 31.15 (C10), 33.53 (C7″), 36.64 (C3″), 46.53 (C3′), 56.00, 56.45, 65.87, 66.20, 71.73, 72.26 (OCH_3, C7,9,14,4′,5′), 98.84 (C1′), 110.36, 110.42 (C5a,-11a), 118.80, 119.56, 119.79 (C1,3,4a), 134.26 (C1″a/1″b), 134.50, 135.67, 136.03, 136.30 (C2,6a,10a,12a), 152.63, 154.19, 156.37 (C6,11,13), 160.65 (C4), 170.83 (C2″a/2″b), 173.75 (C8″), 186.20, 186.27 (C5,12).

4. HPLC (Symmetry C18, 495 nm): purity >95%. ESI-MS (4.0 kV, methanol): *m*/z (%) 779.2 ([M + H]$^+$, 100). ^{13}C NMR (DMSO-d_6): δ 16.75 (C6′), 22.71, 23.91, 25.87, 27.78, 28.32, 28.64 (C2′,4″-8″), 31.07 (C10), 33.72 (C9″), 36.85 (C3″), 46.54 (C3′), 55.99, 56.47, 65.87, 66.24, 71.86, 72.32 (OCH_3, C7,9,-14,4′,5′), 98.84 (C1′), 110.31, 110.41 (C5a,11a), 118.82, 119.55, 119.82 (C1,3,4a), 134.33 (C1″a/1″b), 134.53, 135.67, 136.07, 136.66 (C2,6a,10a,12a), 152.37, 154.19, 156.47 (C6,11,13), 160.69 (C4), 170.94 (C2″a/2″b), 173.91 (C10″), 186.21, 186.27 (C5,12).

5. HPLC (Symmetry C18, 495 nm): purity >95%. ESI-MS (4.0 kV, methanol): *m*/z (%) 753.3 ([M + H]$^+$, 100). ^{13}C NMR (DMSO-d_6): δ 16.73 (C6′), 26.11, 27.04, 27.88, 28.46, 28.73 (C2′,4″-6″,1″a/1″b), 31.06 (C10), 33.82 (C9″), 37.68 (C3″), 46.53 (C3′), 55.91, 56.51, 65.88, 66.24, 71.05, 72.40 (OCH_3, C7,9,-14,4′,5′), 98.83 (C1′), 110.36, 110.49 (C5a,11a), 118.90, 119.63, 119.93 (C1,3,4a), 134.65, 135.68, 136.18, 136.87 (C2,6a,10a,-12a), 152.13, 154.16, 156.49 (C6,11,13), 160.76 (C4), 173.91 (C8″), 177.64 (C2″a/2″b), 186.34, 186.40 (C5,12).

C. Methods. C.1. Fluorescence Polarization. Fluorescence polarization measurements were carried out with black 96-well Greiner microplates (Fluotrac 200) on a Perkin-Elmer Victor^2 V 1420 multilabel HTS counter in fluorescence polarization mode (excitation filter, 485 nm; emission filter, 535 nm; measurement time, 0.5 s per well). The following stock solutions were used: 150 μM HSA in 0.15 M NaCl, 0.004 M sodium phosphate (pH 7.4) with or without 5 equiv of myristic acid. The cysteine-34 position of HSA was blocked by preincubating the stock solution for 2 h with 3 equiv of *N*-ethylmaleimide. **1**−**4** were dissolved in anhydrous methanol at c = 1500 μM. A total of 195 μL of the HSA stock solutions was transferred to a 96-well plate, and an amount of 5 μL of the stock solution of **1**−**4** was added in triplicate to each well. The first fluorescence measurement was performed after 2 min and then every 2 min for 150−360 min at room temperature. Binding curves were obtained by plotting the change in fluorescence polarization (mP) against time (origin 5.0). The mP value for **1**−**4** that was measured with the HSA that was

blocked with *N*-ethylmaleimide was chosen as the zero time value in order to account for the viscosity of the protein solution as well as possible physical interactions with HSA. Second-order rate constants were determined using the following equation:

$$\frac{1}{[\text{HSA}-\text{SH}][\mathbf{1}-\mathbf{4}]} \ln \frac{[\mathbf{1}-\mathbf{4}]([\text{HSA}-\text{SH}] - x)}{[\text{HSA}-\text{SH}]([\mathbf{1}-\mathbf{4}] - x)} = k_2 t$$

with [HSA−SH] = 50 μM, [**1**−**4**] = 37.5 μM, and x = amount of HSA−SH and **1**−**4** that have reacted from $t = 0$ min to $t =$ 150 min.

C.2. Molecular Modeling. C.2.1. FlexX Docking. The hexylmaleimide spacer was docked at the X-ray coordinates of human serum albumin (PDB entry 1BJ5) using the program FlexX 1.8 (42). The "active site" was defined to include any amino acid closer than 10 Å from Cys 34. Standard parameters of the FlexX 1.8 program as implemented in the 6.62 release of the SYBYL package[43] were used for iterative growing and subsequent scoring of FlexX poses. From the top 30 retained solutions, the pose in which the carbon atoms of the maleimide double bond came closest to the thiol group of Cys 34 was chosen.

C.2.2. Parametrization of the Hexylmaleimide-Linked Cys 34 Group. The hexylmaleimide-linked Cys 34 group was first parametrized for the Amber 6.0 program[44] using the AMBER95 force field.[45] Atomic charges were calculated using the Gaussian 94 package[46] and the HF/6-31G* basis set. Therein, atom-centered charges were fitted to an ab initio electrostatic potential using the RESP method[47] under a previously described protocol.[48]

C.2.3. AMBER Minimization and Dynamics. The docked hexylmaleimide was covalently linked to Cys 34. Minimization and dynamics were carried out with AMBER 6.0,[44] using the AMBER95 force field.[45] The minimization was carried out in two steps: first in vacuo, then in a water shell. The minimization in vacuo was carried out with 1000 steps of steepest descent followed by conjugate gradient minimization until the rms gradient of the potential energy was less than 0.25 kcal mol^{-1} Å^{-1}. A twin cutoff (10.0, 15.0 Å) was used to calculate nonbonded electrostatic interactions at every minimization step, and the nonbonded pair list was updated every 25 steps. A distance-dependent ($\epsilon = 4r$) dielectric function was used. For the second minimization, a 25 Å radius water shell was centered around the maleimide. The minimization was then carried out with 1000 steps of steepest descent followed by conjugate gradient minimization until the rms gradient of the potential energy was less than 0.05 kcal mol^{-1} Å^{-1}. Again, a twin cutoff (10.0, 15.0 Å) was used to calculate nonbonded electrostatic interactions at every minimization step and the nonbonded pair list was updated every 25 steps. A dielectric constant of $\epsilon = 1$ was used. Only the covalently linked maleimide spacer and the amino acids completely surrounded by water were allowed to move ("belly" option of AMBER). Starting from the minimized structure, a molecular dynamics simulation of the solvated complex was carried out over 100 ps. A time step of 1 fs was used. Twin cutoff, dielectric constant, and belly option were set as for the second minimization.

C.2.4. Docking of Doxorubicin. Starting from the time-averaged coordinates of the HSA−maleimide complex, doxorubicin was manually linked to the hexyl spacer via a hydrazone moiety to form **3**. The conformations of the hydrazone linker and doxorubicin were manually adjusted to optimize, as far as possible, their interactions with HSA.

C.3. HPLC Studies. HPLC was performed with a Waters system (pump, Waters 616; detector, Waters 996 photodiode array detector and a Merck F-1050 fluorescence spectrophotometer; controller, Waters 600S; auto sampler, Waters 717; software, Millenium, version 2.10; column, Waters, 300 Å, Symmetry C18 [4.6 mm × 250 mm] with precolumn). The chromatographic conditions were the following: flow, 1.2 mL/min; mobile phase, 27.5% CH_3CN, 72.5% 20 mM potassium phosphate (pH 7.0); mobile phase B, CH_3CN; gradient, 0−25 min 100% mobile phase; 25−40 min increase to 70% CH_3CN, 30% 20 mM potassium phosphate; 40−50 min 70% CH_3CN, 30% 20 mM potassium phosphate; 50−60 min decrease to initial mobile phase; injection volume, 50 μL.

C.4. Synthesis of the Albumin Conjugate of 3. A total of 2.0 g of human serum albumin (10 mL of a 20% solution from Pharma Dessau) was diluted with 10 mL of 0.004 M sodium phosphate, 0.15 M NaCl buffer (pH 7.4) to which 0.4 equiv of **3** was added, and the solution was incubated at room temperature for 3 h. The albumin conjugate was obtained by subsequent size-exclusion chromatography (Sephadex G.25; buffer 0.004 M sodium phosphate, 0.15 M NaCl (pH 7.4)) using a LKB 8300-UVCORD monitor (280 nm) controlled by FPLC detector software (version 1.03, Pharmacia Biotech, Uppsala, Sweden). The content of anthracycline in the sample was determined using the ϵ value for **3** that was determined as ϵ_{495}(pH 7.4) = 9250 M^{-1} cm^{-1}. The concentration of **3** in the conjugate was adjusted to 500 ± 50 μM by concentrating the sample with CENTRIPREP-10 concentrators from Amicon, FRG (4 °C and 4500 rpm). Samples were kept frozen at −78 °C and thawed prior to use.

C.5. Incubation Studies with Human Serum Albumin. Doxorubicin, **3**, or **5** was added to a 700 μM solution of human serum albumin (buffer: 0.15 M NaCl, 4 mM sodium phosphate (pH 7.4)) at 37 °C at a final concentration of 100 μM, and the sample was incubated for 5 or 90 min and for 24 h. A 50 μL sample was analyzed by HPLC.

C.6. Incubation Studies with Human Plasma. Human blood plasma (EDTA-stabilized) was taken from healthy volunteers. Doxorubicin, **3**, or **5** was added to plasma preincubated at 37 °C at a final concentration of 100 μM, and the samples were incubated for 2, 5, or 90 min and for 24 h at 37 °C. A 50 μL sample was analyzed by HPLC.

C.7. Incubation Studies with Human Blood. Human blood (EDTA-stabilized) was taken from healthy volunteers. Doxorubicin or **3** was added to a human blood sample to a final concentration of 225 μM (fresh blood samples were stabilized with EDTA and preincubated at 37 °C). After an incubation time of $t = 0$, 1, 2, 3, 5, 6, 10, 30, and 60 min and 24 h, 1.2 mL of each sample was centrifuged in a 2 mL Eppendorf reaction tube at a maximum of 7500 rpm/min (duration: 20−30 s). Plasma samples (50 μL) were analyzed by reverse-phase HPLC or an amount of 3 × 100 μL of the plasma phase was diluted with 700 μL of sodium phosphate buffer (4 mM sodium phosphate, 0.15 M NaCl, pH 7.4) and the concentration of anthracycline was measured photometrically at 495 nm against a plasma reference without the drug. The average of three absorption values at 495 nm is depicted in Figure 10 against the time scale.

C.8. Incubation Studies of the Albumin Conjugate of 3 at pH 5.0. The pH value of the albumin conjugate of **3**, dissolved in 4 mM sodium phosphate, 0.15 M NaCl, pH 7.4, was adjusted to pH 5.0 with 0.02 M sodium acetate (pH 3.0), and 100 μM samples were incubated at 37 °C. Samples (50 μL) were analyzed by HPLC at $t = 0$, 10, 20, 30, 40, 50, 60, 90, and 180 min. The decrease in the ratio of the peak size of the conjugate at 495 to that at 280 nm with time was used as a measure of the acid lability of the albumin-bound form of **3**.

C.9. Determination of Intracellularly Released Doxorubicin. The albumin conjugate of **3** (20 μM) was incubated with approximately 500 000 MCF-7 tumor cells for 6, 16, and 24 h in 4−6 culture dishes. Subsequently, the number of cells were counted. Cells from the remaining dishes were washed three times with ice-cold phosphate-buffered saline and were recovered in 250 μL of cold PBS using a cell scraper. The cell suspension was then ultrasonicated (100 W) for 3 min. To 250 μL of this suspension was added 300 μL of a 0.1 M sodium borate buffer (pH 9.2) and 900 μL of a 4:1 mixture of chloroform and methanol to extract the drug. The tube was vigorously shaken (3 min) and centrifuged (2 min), and the organic layer was collected and evaporated in high vacuum. The residue was dissolved in 250 μL of mobile phase, and a 200 μL sample was injected on a Symmetry C-18 column using fluorescence detection (EX 480, EM 550) as described above.

C.10. Cell Culture. LXFL 529, MCF-7, and RENCA cells were grown as monolayer cultures in cell culture flasks (Greiner Labortechnik, Frickenhausen, FRG) in RPMI 1640 culture medium with phenol red supplemented with 10% heat-inactivated FCS, 100 μg/mL glutamine, 100 U/mL penicillin, and 100 μg/mL streptomycin.

Carcinoma cells were cultured at 37 °C in a humidified atmosphere of 95% air and 5% carbon dioxide at 37 °C. Media were routinely changed every 3 days. For subculture or experiments, cells growing as monolayer cultures were released from the tissue flasks by treatment with 0.05% trypsine/EDTA, and viability was monitored using the cell analyzer system Casy 1 from Schärfe Systems (Reutlingen, FRG). For the experiments, cells were used during the logarithmic growth phase.

C.11. BrdU-Incorporation Assay. The 5-bromo-2′-deoxyuridine cell proliferation kit (catalogue no. 1647229) was obtained from Boehringer Mannheim (Mannheim, FRG). To determine the index of DNA synthesis, BrdU was measured according to the instructions of the manufacturer. Briefly, $(1.0-1.2) \times 10^4$ cells/cm^2 were plated in each well of a 96-well tissue culture plate. Medium supplemented with 10% FCS was added, and cells were allowed to adhere for 24 h. Subsequently, cells were preincubated with various drug concentrations for 36 h and were then labeled by adding 10 mM BrdU to each well. Cultures were incubated in the presence of BrdU for 12 h. After this period, cells were fixed with FixDenat solution at room temperature (RT) for 30 min, washed three times with washing solution at RT, and incubated with a monoclonal anti-BrdU-peroxidase Fab fragment (diluted 1:10000 with PBS) for 90 min at RT. DNA was then washed three times with washing solution at RT, and incorporated BrdU was visualized by adding 100 μL of the peroxidase substrate BM blue. After an incubation time of 10 min, the extinction of the samples was quantified with an ELISA reader (Dynatech Laboratories Inc., Sullyfield, U.K.) at a wavelength of 405 nm and set as the index of DNA synthesis. Four separate cultures were determined per concentration. Results are shown as means ± SD ($n = 4$). Similar results were obtained in a further separate experiment.

C.12. Animal Experiments. C.12.1. RENCA Model. All animal experiments were carried out according to the guidelines of the Ethical Committee of the Regierungspräsidium, Freiburg, FRG. The animals were female BALB/c mice routinely used at 6−8 weeks of age (approximate weight of 20 g). RENCA is a tumor that arose spontaneously in the kidney of BALB/c mice and can be cultured in vitro. Histologically, RENCA consists of granular cell type adenocarcinoma that are pleomorphic with large nuclei. The murine RENCA cell line was maintained in vitro in RPMI 1640 medium supplemented with 10% FCS and 1% P/S (penicillin/streptomycin) in a 5% CO_2 incubator. The injection of 10^6 RENCA cells in 0.2 mL aliquots into the subcapsular space of the left kidney was performed through a flank incision after the animals were anesthetized with 0.5−1.5 vol % isoflurane, which is used in combination with an oxygen flow of 1.5 L. The subcapsular renal injection of 10^6 RENCA cells in a syngenic BALB/c mouse is followed by the progressive development of a primary tumor mass in the left kidney. One week after application, the primary tumor is macroscopically visible. After 10 days, spontaneous metastases generally develop in the regional lymph nodes and in the lung, peritoneum, and liver, allowing RENCA to be staged similarly to human renal cell carcinoma. The mean survival time of RENCA-bearing mice is approximately 46 days when injecting 10^6 RENCA cells.

C.12.2. Therapy. Twelve animals per group were used for the experiment. Therapy was initiated by intravenous application of a single dose of 10 μmol mg kg^{-1} doxorubicin and 10 μmol mg kg^{-1} or 20 μmol/kg of **3** on days 10, 13, 17, and 20 after renal application of RENCA cells (day 1). Animal weight was taken every other day. The animals were sacrificed on day 24, and primary tumor size and weight were determined.

C.12.3. Xenograft Experiments. For the in vivo testing of **3** in comparison with doxorubicin female Ncr:nu/nu mice (Taconic breeding facility, Germantown) were used. The mice were held in laminar flow shelves under sterile and standardized environmental conditions (25 ± 2 °C room temperature, 50 ± 10% relative humidity, 12 h light−dark rhythm). They received autoclaved food and bedding (ssniff, Soest, Germany) and acidified (pH 4.0) drinking water ad libitum. All animal experiments were performed under the auspices of the German animal protection law.

The breast carcinoma cell lines MDA-MB-435 and MCF-7 were a kind gift from the tumor bank of the NCI. One in vivo growing tumor was taken and cut into pieces of 2−3 mm diameter. Fragments were transplanted subcutaneously (sc) into the left flank region of anaesthetized (40 mg/kg ip, Radenarkon, Asta Medica, Frankfurt, Germany) mice on day zero. Mice were randomly distributed into the experimental groups. When the tumors were grown to a palpable size (4−5 mm diameter), treatment was initiated (see Figures 15 and 16). Mice were treated intravenously weekly with either saline, doxorubicin, or **3** (for doses and schedules, see corresponding tables and figures). The volume of administration was 0.2 mL per 20 g of body weight.

Tumor size was measured twice weekly with a caliper-like instrument in two dimensions. Individual tumor volumes (V) were calculated by the formula $V = (\text{length} + [\text{width}]^2)/2$ and referenced to the values on the first day of treatment (relative tumor volume, RTV). At each measurement day, treated/control values (T/C) were calculated as a percentage for each experimental group. The optimum (lowest) values obtained within 4 weeks after treatment were used for evaluating the efficacy of the compounds, and optimum T/C values are presented in the respective tables. The body weight of mice was determined twice weekly and referenced to the body weight on the first day of treatment (body weight change, BWC). The maximum change in body weight after initiation of treatment is presented in the respective tables.

Acknowledgment. The support of the Dr. Mildred-Scheel Stiftung der Deutschen Krebshilfe is gratefully acknowledged.

Supporting Information Available: Figures 3, 6, 8, 9, 11−14, and 18−21 and Tables 3 and 4. This material is available free of charge via the Internet at http://pubs.acs.org.

References

(1) Dorr, R. T.; Von Hoff, D. D. *Cancer Chemotherapy Handbook*, 2nd ed.; Appleton and Lange: Norwalk, CT, 1994.
(2) Myers, C. E.; Chabner, B. A. Anthracyclins. In *Cancer Chemotherapy—Principles and Practice*; Chabner, B. A., Collins, J. M., Eds.; Lippincott: Philadelphia, 1990; pp 356−381.
(3) Takakura, Y.; Hashida, M. Macromolecular drug carrier systems in cancer chemotherapy: macromolecular prodrugs. *Crit. Rev. Oncol. Hematol.* **1994**, *18*, 207−231.
(4) Kratz, F.; Warnecke, A.; Rodrigues, P. C. A.; Riebeseel, K. Anticancer Drug Conjugates with Macromolecular Carriers. In *Polymeric Biomaterials*, 2nd ed.; Dumitriu, S., Ed.; Marcel Dekker: New York, 2002; Chapter 32, pp 851−894.
(5) Kratz, F.; Beyer, U. Serum proteins as drug carriers of anticancer agents, a review. *Drug Delivery* **1998**, *5*, 1−19.
(6) Kratz, F.; Beyer, U.; Roth, T.; Tarasova, N.; Collery, P.; Lechenault, F.; Cazabat, A.; Schumacher, P.; Unger, C.; Falken, U. Transferrin conjugates of doxorubicin: synthesis, characterization, cellular uptake, and in vitro efficacy. *J. Pharm. Sci.* **1998**, *87*, 338−346.
(7) Kratz, F.; Beyer, U.; Collery, P.; Lechenault, F.; Cazabat, A.; Schumacher, P.; Falken, U.; Unger, C. Preparation, characterization and in vitro efficacy of albumin conjugates of doxorubicin. *Biol. Pharm. Bull.* **1998**, *21*, 56−61.
(8) Kratz, F.; Beyer, U.; Schumacher, P.; Krüger, M.; Zahn, H.; Roth, T.; Fiebig, H. H.; Unger, C. Synthesis of new maleimide derivatives of daunorubicin and biological activity of acid-labile transferrin conjugates. *Bioorg. Med. Chem. Lett.* **1997**, *7*, 617−622.
(9) Kratz, F.; Fichtner, I.; Roth, T.; Fiebig, H. H.; Unger, C. Antitumor activity of acid-sensitive transferrin and albumin doxorubicin conjugates in in vitro and in vivo human tumor xenograft models. *J. Drug Targeting* **2000**, *8*, 305−318.
(10) Drevs, J.; Hofmann, I.; Marmé, D.; Unger, C.; Kratz, F. In vivo and in vitro efficacy of an acid-sensitive albumin conjugate of doxorubicin compared to the parent compound in murine renal cell carcinoma. *Drug Delivery* **1999**, *6*, 1−7.

(11) Kratz, F.; Müller-Driver, R.; Hofmann, I.; Drevs, J.; Unger, C. A Novel Macromolecular Prodrug Concept Exploiting Endogenous Serum Albumin as a Drug Carrier for Cancer Chemotherapy. *J. Med. Chem.* **2000**, *43*, 1253−1256.
(12) Sogami, M.; Era, S.; Nagaoka, S.; Kuwata, K.; Kida, K.; Miura, H.; Inoue, E.; Hayano, Sawada, S.; Noguchi, K.; Miyata, S. High-performance liquid chromatographic studies on non-mercapt in equilibrium with mercapt conversion of human serum albumin. *J. Chromatogr.* **1985**, *332*, 19−27.
(13) Etoh, T.; Miyazahi, M.; Harada, K.; Nakayama, M.; Sugii, A. Rapid analysis of human serum albumin by high-performance liquid chromatography. *J. Chromatogr.* **1992**, *578*, 292−296.
(14) Era, S.; Hamaguchi, T.; Sogami, M.; Kuwata, K.; Suzuki, E.; Miura, K.; Kawai, K.; Kitazawa, Y.; Okabe, H.; Noma, A.; Miyata, S. Further studies on the resolution of human mercapt- and nonmercaptalbumin and on human serum albumin in the elderly by high-performance liquid chromatography. *Int. J. Pept. Protein Res.* **1988**, *31*, 435−442.
(15) Coleman, R. D.; Kim, T. W.; Gotto, A. M.; Yang, C. Determination of cysteine on low-density lipoprotein using the fluorescent probe, 5-iodoacetamidofluoresceine. *Biochim. Biophys. Acta* **1990**, *1037*, 129−132.
(16) Ferguson, E.; Singh, R. J.; Hogg, N.; Kalyanaraman, B. The mechanism of apolipoprotein B-100 thiol depletion during oxidative modification of low-density lipoprotein. *Arch. Biochem. Biophys.* **1997**, *341*, 287−294.
(17) Yang, C.; Kim, T. W.; Wenig, S.; Lee, B.; Yang, M.; Gotto, A. M. Isolation and characterization of sulfhydryl and disulphide peptides of human apolipoprotein B-100. *Proc. Natl. Acad. Sci. U.S.A.* **1990**, *87*, 5523−5527.
(18) Smith, D. E.; Mosher, D. F.; Johnson, R, B.; Furcht, L. T. Immunological identification of two sulfhydryl-containing fragments of human plasma fibronectin. *J. Biol. Chem.* **1982**, *260*, 5831−583.
(19) Narasimhan, C.; Lai, C.-S. Differential behavior of the two free sulfhydryl groups of human plasma fibronectin: effects of environmental factor. *Biopolymers* **1991**, *31*, 1159−1170.
(20) Shimokawa, Y.; Abe, O.; Kuromizu, K. Fluorescence labeling of a single sulfhydryl group in human plasma α_1-proteinase inhibitor and characterization of the labeled inhibitor. *J. Biochem.* **1986**, *100*, 563−570.
(21) Morii, M.; Odani, S.; Koide, T.; Ikenaka, T. Human α_1-antitrypsin−characterization of N- and C-terminal sequences. *J. Biochem.* **1978**, *83*, 269−277.
(22) Putnum, F. W. In *The Plasma Proteins*, 2nd ed.; Putman, F. W., Ed.; Academic Press: New York; Vol. 4, pp 76−86.
(23) Mansoor, M. A.; Svardal, A. M.; Ueland, P. M. Determination of the in vivo redox status of cysteine, cysteinylglycine, homocysteine, and glutathione in human plasma. *Anal. Biochem.* **1992**, *200*, 218−229.
(24) Müller, F.; Svardal, A. M.; Aukrust, P.; Berge, R. K.; Ueland, P. M.; Froland, S. S. Elevated plasma concentration of reduced homocysteine in patients with human immunodeficiency virus infection. *Am. J. Clin. Nutr.* **1996**, *63*, 242−248.
(25) Hagenfeldt, B.; Arvidsson, L.; Larsson, A. Glutathione and γ-glutamylcysteine in whole blood, plasma and erythrocytes. *Clin. Chim. Acta* **1978**, *85*, 167−173.
(26) Martensson, J. The effect of fasting on leukocyte and plasma glutathione and sulfur amino acid concentrations. *Metabolism* **1986**, *35*, 118−121.
(27) Hulea, S. A.; Olinescu, R.; Nita, S.; Crocnan, D.; Kummerow, F. A. Cigarette smoking causes biochemical changes in blood that are suggestive of oxidative stress: a case-control study. *J. Environ. Pathol., Toxicol. Oncol.* **1995**, *14*, 173−180.
(28) Hack, V.; Breitkreutz, R.; Kinscherf, R.; Röhrer, H.; Bärtsch, P.; Tau, F.; Benner, A.; Dröge, W. The redox state as a correlate of senescence and wasting and as a target for therapeutic intervention. *Blood* **1998**, *92*, 59−67.
(29) Pedersen, A.; Jacobsen, J. Reactivity of the thiol group in human and bovine albumin at pH 3−9, as measured by exchange with 2,2′-dithiopyridine. *Eur. J. Biochem.* **1980**, *106*, 291−295.
(30) Carter, D. C.; Ho, J. X. Structure of serum albumin. *Adv. Protein Chem.* **1994**, *45*, 153−203.
(31) Krüger, M.; Beyer, U.; Schumacher, P.; Unger, C.; Zahn, H.; Kratz, F. Synthesis and stability of four maleimide derivatives of the anticancer drug doxorubicin for the preparation of chemoimmunoconjugates. *Chem. Pharm. Bull.* **1997**, *47*, 399−401.
(32) Beyer, U.; Krüger, M.; Schumacher, P.; Unger, C.; Kratz, F. Synthese von Bifunktionellen Maleinimidverbindungen zur Herstellung von Chemoimmunokonjugaten. *Monatsh. Chem.* **1997**, *128*, 91−102.
(33) Tournier, E. J. M.; Wallach, J.; Blond, P. Sulfosuccinimidyl 4-(*N*-maleimidomethyl)-1-cyclohexane carboxylate as a bifunctional immobilization agent. Optimization of the coupling conditions. *Anal. Chim. Acta* **1998**, *361*, 33−44.
(34) Maeda, H.; Wu, J.; Sawa, T.; Matsumura, Y.; Hori, K. Tumor vascular permeability and the EPR effect in macromolecular therapeutics: A review. *J. Controlled Release* **2000**, *65*, 271−284.
(35) Vasey, P. A.; Kaye, S.-B.; Morrison, R.; Twelves, C.; Wilson, P.; Duncan, R.; Thomson, H.; Murray, L. S.; Hilditch, T. E.; Murray, T.; Burtles, S.; Fraier, D.; Frigerio, E.; Cassidy, J. Phase I clinical and pharmacokinetic study of PK1 [*N*-(2-hydroxypropyl)methacrylamide copolymer doxorubicin]: first member of a new class of chemotherapeutic agents−drug polymer conjugates. *Clin. Cancer. Res.* **1999**, *5*, 83−94.
(36) Greenwald, R. B.; Conover, C. D.; Choe, Y. H. Poly(ethylene glycol) conjugated drugs and prodrugs: A comprehensive review. *Crit. Rev. Ther. Drug Carrier Syst.* **2000**, *17*, 101−161.
(37) Willner, D.; Trail, P. A.; Hofstead, S. J.; King, H. D.; Lasch, S. J.; Braslawsky, G. R.; Greenfield, R. S.; Kaneko, T.; Firestone, R. A. (6-Maleimidocaproyl)hydrazone of doxorubicin−A new derivative for the preparation of immunoconjugates of doxorubicin. *Bioconjugate Chem.* **1993**, *4*, 521−527.
(38) Trail, P. A.; Willner, D.; Lasch, S. J.; Hernderson, A. J.; Hofstead, S.; Casazza, A. M.; Firestone, R. A.; Hellström, I.; Hellström, K. E. Cure of xenografted human carcinomas by BR96-doxorubicin immunoconjugates. *Science* **1993**, *261*, 212−215.
(39) Beyer, U.; Rothen-Rutishauser, B.; Unger, C.; Wunderli-Allenspach, H.; Kratz, F. Differences in the Intracellular Distribution of Acid-Sensitive Doxorubicin−Protein Conjugates in Comparison to Free and Liposomal Formulated Doxorubicin as Shown by Confocal Microscopy. *Pharm. Res.* **2001**, *18*, 29−38.
(40) Trail, P. A.; Willner, D.; Knipe, J.; Henderson, A. J.; Lasch, S. J.; Zoeckler, M. E.; TrailSmith, M. D.; Doyle, T. W.; King, H. D.; Casazza, A. M.; Braslawsky, G. R.; Brown, J.; Hofstead, S. J.; Greenfield, R. S.; Firestone, R. A.; Mosure, K.; Kadow, K. F.; Yang, M. B.; Hellström, K. E.; Hellström, I. Effect of linker variation on the stability, potency, and efficacy of carcinoma-reactive BR64-doxorubicin immunoconjugates. *Cancer Res.* **1997**, *57*, 100−105.
(41) Tolcher, A. W.; Sugarman, S.; Gelman, K. A.; Cohen, R.; Saleh, M.; Isaacs, C.; Young, L.; Healy, D.; Onetto, N.; Slichenmyer, W. Randomized phase II study of BR96-doxorubicin conjugate in patients with metastatic breast cancer. *J. Clin. Oncol.* **1999**, *2*, 478−484.
(42) Rarey, M.; Kramer, B.; Lengauer, T.; Klebe, G. A fast flexible docking method using an incremental construction algorithm. *J. Mol. Biol.* **1996**, *261*, 470−489.
(43) *SYBYL*. version 6.62; Tripos Inc., St. Louis, MO 63144.
(44) Case, D. A.; Pearlman, D. A.; Caldwell, J. W.; Cheatham, T. E., III; Ross, W. S.; Simmerling, C. L.; Darden, T. A.; Merz, K. M.; Stanton, R. V.; Cheng, A. L.; Vincent, J. J.; Crowley, M.; Tsui, V.; Radmer, R. J.; Duan, Y.; Pitera, J.; Massova, I.; Seibel, G. L.; Singh, U. C.; Weiner, P. K.; Kollman, P. A. *AMBER 6*; University of California: San Francisco, CA, 1999.
(45) Cornel, W. D.; Cieplak, P.; Bayly, C. I.; Gould, I. R.; Merz, J. K. M.; Ferguson, D. M.; Spellmeyer, D. M.; Fox, T.; Caldwell, J. W.; Kollman, P. A. A second generation force field for the simulation of proteins, nucleic acids, and organic molecules. *J. Am. Chem. Soc.* **1995**, *117*, 5179−5197.
(46) Frisch, M. J.; Trucks, G. W.; Schlegel, H. B.; Gill, P. M. W.; Johnson, B. G.; Robb, M. A.; Cheeseman, J. R.; Keith, T.; Petersson, G. A.; Montgomery, J. A.; Raghavachari, K.; Al-Laham, M. A.; Zakrzewski, V. G.; Ortiz, J. V.; Foresman, J. B.; Cioslowski, J.; Stefanov, B. B.; Nanayakkara, A.; Challacombe, M.; Peng, C. Y.; Ayala, P. Y.; Chen, W.; Wong, M. W.; Andres, J. L.; Replogle, E. S.; Gomperts, R.; Martin, R. L.; Fox, D. J.; Binkley, J. S.; Defrees, D. J.; Baker, J.; Stewart, J. P.; Head-Gordon, M.; Gonzalez, C.; Pople, J. A. *Gaussian 94*, revision C.3; Gaussian, Inc.: Pittsburgh, PA, 1995.
(47) Bayly, C. I.; Cieplak, P.; Cornell, W. D.; Kollman, P. A. A well-behaved electrostatic potential based method using charge restraints for determining atom-centered charges: The RESP model. *J. Phys. Chem.* **1993**, *97*, 10269−10280.
(48) Cieplak, P.; Cornell, W. D.; Bayly, C. I.; Kollman, P. A. Application of the Multimolecule and Multiconformational RESP Methodology to Biopolymers: Charge Derivation for DNA, RNA, and Proteins. *J. Comput. Chem.* **1995**, *16*, 1357−1377.

JM020276C